MACEIÓ - ALAGOAS
EBA 15
15° ENCONTRO BRASILEIRO SOBRE ADSORÇÃO
15th Brazilian Meeting about Adsorption

Novel Adsorbents from Acrocomia Totai Leaves for Caffeine Removal: A Sustainable Approach

Rogerio S. Maniezzo[a,b†], Hugo H. C. de Lima[a,b] , Gredson Keiff Souza[c], Armando Mateus Pomini[c], Andrelson Wellington Rinaldi[a,b,*]

[a] *Rinaldi Research Group, Universidade Estadual de Maringá, Av. Colombo, 5790 Bloco 15 – Maringá – PR 87020-900 Brazil*
[b] *Marili Hidrocarvões Ativados, Av. Colombo,5790 Bloco 15 – Maringá – PR – 87020-900 Brazil*
[c] *Departamento de Química, Universidade Estadual de Maringá, Av. Colombo, 5790 Bloco 26 sl.05 – Maringá – PR 87020-900 Brazil*

†rsmaniezzo@gmail.com * awrinaldi@uem.br

Abstract

This study focused on the production of activated hydrochars from Acrocomia Totai leaves. The hydrochars were synthesized through hydrocarbonization with KOH in a ratio of 1:5 (m/m). The specific surface area (SBET) was determined to be 2.132 $m^2.g^{-1}$ for HDML-ATV, 1726 $m^2.g^{-1}$ for HME4h-ATV and 1.735 $m^2.g^{-1}$ for HME48h-ATV. Regarding the maximum amount adsorbed, the hydrochars gave the following results: 411.78 mg g^{-1} for HMDL-ATV, 344.52 mg g^{-1} for HME4h-ATV, and 303.43mgg-1 for HME48h-ATV. The results of this study demonstrate the potential of using Acrocomia Totai leaves for the production of activated hydrochars with large surface areas, which can be used for various applications, including the adsorption of caffeine (CFN).

Keywords: Hydrochars; Caffeine adsorption; Green chemistry; Acrocomia totai leaves.

1. Introduction

The macauba palm, native to Brazil, is known for its versatile uses[1]. Its leaves are used for biocomposite materials, while the seeds are used for biofuel production. The production of porous materials from macauba is of particular interest, as it offers a sustainable alternative for various applications[2]. The leaves and seeds are rich in cellulose and lignin, making them suitable for the production of porous materials such as activated carbon and biochar. These materials have a wide range of uses, including water filtration, air purification, and as a substrate for catalytic reactions. The use of macauba for the production of porous materials aligns with the growing demand for sustainable and eco-friendly alternatives in various industries.

2. Synthesis of hydrochars

This study focused on Macaúba palm trees from Moreira Sales, Paraná, Brazil (latitude -24º 3' 23.64", longitude -53º 3' 26.32"), selected as the raw material for hydrochar production. Three samples were collected: one from fallen burlap and two from lipid-extracted Macaúba using a Soxhlet apparatus for either 4 or 48 [3].

Hydrochar was produced via hydrocarbonization by placing 5.00 g. of each sample in a Teflon®-lined stainless steel autoclave with 37 mL of deionized water, heated to 190ºC for 48 hours. The resulting hydrochars were dried at 70ºC for 12 hours and labeled as HMDL (burlap-derived), HME4h (4-hour lipid extraction), and HME48h (48-hour lipid extraction).

2.1 Chemical activation of hydrochars.

Samples were chemically activated with KOH (1:5 ratio), mixed with deionized water, stirred, and heated to 800ºC in argon gas. Post-activation, samples were washed with deionized water and 0.1 M HCl, then dried at 100ºC for 12 hours.

2.2 Characterization of hydrochars and activated hydrochars

Nitrogen physisorption isotherms at 77 K for activated hydrochars were measured using a QuantaChrome Nova 1200e, with BET surface

areas (S_{BET}) from 0.05–0.20 relative pressure. Total pore volume (V_T) was determined at p/p_o = 0.99. FTIR-ATR and Raman spectra were recorded using Bruker spectrophotometers, while SEM evaluated morphological features.

2.4 Adsorption studies

Adsorption studies used 20.0 mL CFN solutions and 10 mg activated hydrochars in 50 mL flasks, shaken at 70 rpm and 25°C. CFN concentrations were measured with a Cary 50 spectrophotometer after 0.44 µm vacuum filtration. The effects of pH (3.0-11.0), time (0-480 min), and adsorption isotherms (100-500 mg/L CFN, pH 7.0) were evaluated using Langmuir, Freundlich, Dubinin-Radushkevich, and Redlich-Peterson models.

The maximum CFN amounts adsorbed onto activated hydrochars, qe (efect of pH (3.0 - 11.0), adsorption isotherms and temperature effect (25. 45 e 55°C) and the CFN amounts adsorbed at time t, q_t, were determined from Equation 1.

$$q_t = q_e = \frac{(C_0 - C_f)v}{w} \quad (1)$$

Isothermal and kinetic models were fitted to experimental data using a nonlinear equations. The data were processed using Origin® 8.5 software. the normalized standard deviations (Δ_{qe}) (Equation 2) and the correlation coefficiente (R^2) were used to compare the applicability of the CFN adsorption data to the proposed model.

$$\Delta q_e(\%) = 100\sqrt{\sum \frac{\left[\frac{q_{e,\exp} - q_{e,cal}}{q_{e,\exp}}\right]^2}{N-1}} \quad (2)$$

Where $q_{e,exp}$ and $q_{e,cal}$ are experimental and calculated values of the adsorbed amounts, respectively, and N represents the number of experiments.

3. Results and discussions

3.1 Characterization of HM-ATV

The textural properties of HMDL-ATV, HME4h-ATV, and HME48h-ATV are shown in Table 1. HMDL-ATV has a high S_{BET} (2132 m^2g^{-1}) due to the burlap's high carbon content. HME4h-ATV and HME48h-ATV, with extracted compounds where carbon is the major element, have lower S_{BET} values than HMDL-ATV. Additionally, the samples exhibit a high mesopore/micropore volume ratio and an average pore diameter of 2.25 nm. HME4h-ATV and HME48h-ATV have high S_{BET} values of 1726 m^2g^{-1} and 1735 m^2g^{-1}, respectively.

Table 1. Textural properties of HMDL-A TV, HME4h-ATV and HME4h-ATV.

Sample	S_{BET}	V_T	V_{micro}	V_{meso}	D_P
HDML-ATV	2132	1120	0.801	0.319	2.25
HME4h-ATV	1726	0.996	0.672	0.324	3.40
HME48h-ATV	1735	0.974	0.692	0.282	2.24

S_{BET} (m^2g^{-1}); V_T (cm^3g^{-1}); V_{micro} (cm^3g^{-1}); Vmeso(cm^3g^{-1}); Dp(nm).

The SEM images of HMDL-ATV, HME4h-ATV, and HME48h-ATV are shown in Figure 2A, B, and C reveal a dense, irregular morphology without cavities. In contrast, the SEM images of the activated hydrochars display numerous cavities of various structures, formed due to the KOH chemical activation of Macaúba leaves. These cavities on the surface of the activated hydrochars may be responsible for CFN adsorption.

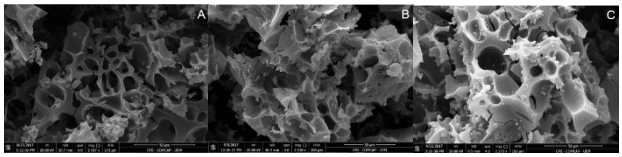

Figure 2- SEM images A- HMDL-ATV, B- HME4h-ATV and HME48h-ATV

Figure 3A shows the FTIR spectra of activated hydrochars, indicating different chemical bonds and functional groups. All materials exhibit similar profiles: −OH stretching in hydroxyl and carboxyl groups (~3600 cm^{-1}), C-H stretching in aliphatic and aromatic structures (~3000 cm^{-1}), and C=C presence (~1650 cm^{-1}). Hydrochars show bands at 1530, 1142, 934, and 521 cm^{-1}, while activated hydrochars reveal new bands at 1340 and 707 cm^{-1}. These findings align with previous studies [4,5].

The Raman spectra of activated hydrochar and hydrochar (Figure 3B) show two bands: D at 1348 cm^{-1} and G at 1591 cm^{-1}. The D band indicates defects, while the G band represents ordered sp^2 carbon. The graphitization degree, determined by the ID/IG ratio, is higher in hydrochar (ID/IG < 0.89) than in activated hydrochar (ID/IG > 0.97), indicating reduced graphitization post-activation.

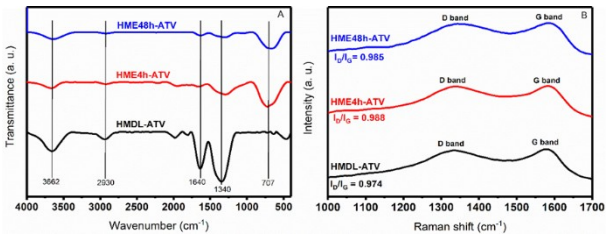

Figure 3 - A- FTIR spectra and B- Raman scattering of activated hydrochars

3.2 Adsorption studies

3.2.1 Adsorption kinetics

Figure 4 shows CFN adsorption kinetics on three activated hydrochars, with rapid increase in the first 120 min, reaching equilibrium at 480 min. High q_{tq} values are seen early. Non-linear kinetic models (pseudo-first order, pseudo-second order, and Elovich) fit the experimental data. Table 3 presents the kinetic parameters.

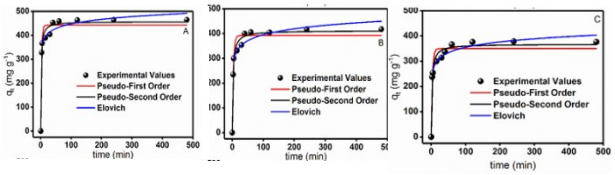

Figure 4 - Adsorption kinetics of CFN on A - HMDL-ATV, B – HME4h-ATV and C – HME48h-ATV

Table 2 shows that the pseudo-second-order model best correlated with the experimental data for HMDL-ATV and HME4h-ATV, while the Elovich model fit HME48h-ATV data best. These models had high R^2 (0.9825, 0.9844, 0.9813) and low standard deviations (Δ_{qe}= 4.43, 6.79, 8.94). Initial adsorption rates confirm quick CFN adsorption, with HMDL-ATV > HME4h-ATV > HME48h-ATV, reflecting their S_{BET} and micropore volume. These properties effectively retain caffeine molecules (dimensions in nm: 1.06 length, 0.85 width, 0.45 thickness).

Table 2. Kinetic parameters of CFN adsorption

Sample	Kinetic parameter			
	Pseudo-First Order			
(I)	q_e=464.50	k_1=0.41	h_0=181.15	R^2=0.9590
(II)	q_e=391.35	k_1=0.28	h_0=109.57	R^2=0.9535
(III)	q_e=349.55	k_1=0.31	h_0=108.36	R^2=0.9312
	Pseudo Second Order			
(I)	q_e=457.09	k_2=0.0016	h_0=334.29	R^2=0.9825
(II)	q_e=411.18	k_2=0.0011	h_0=185.97	R^2=0.9844
(III)	q_e=366.94	k_2=0.0013	h_0=175.13	R^2=0.9744
	Elovich			
(I)	α= 2.64 10^6	β=0.036		R^2=0.9806
(II)	α= 3.04 10^5	β=0.028		R^2=0.9645
(III)	α= 3.38 10^5	β=0.032		R^2=0.9813

q_e (mg g^{-1}); k_1= min^{-1}; h_0= mg g^{-1} min^{-1}; k_2= g mg^{-1} min^{-1}; α = g mg^{-1} min^{-2};β = mg g^{-1} min^{-1} **(I) HDML-ATV; (II) HME4h-ATV; (III) HME48h-ATV**

3.2.2 Adsorption isotherms

The isotherms of caffeine adsorption onto the synthesized activated hydrochars were investigated and are shown in Figure 5. Non-linear isotherm models (Langmuir, Freundlich, Dubinin-Radushkevich, and Redlich-Peterson) and their parameters are displayed in Table 4.

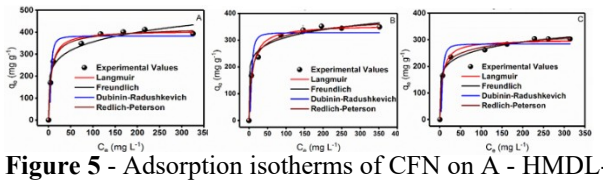

Figure 5 - Adsorption isotherms of CFN on A - HMDL-ATV, B – HME4h-ATV and C – HME48h-ATV

From the adsorption isotherm , the maximum CFN adsorption capacities onto activated hydrochars were determined: 411.78 mg g^{-1} for HMDL-ATV, 344.52 mg g^{-1} for HME4h-ATV, and 303.43mgg^{-1} for HME48h-ATV [6]. Langmuir and Redlich-Peterson models showed the best correlation, with high R^2 values and low Δ_{qe} The Langmuir model estimated close to experimental monolayer adsorption capacities (q_{max}), suggesting homogeneous adsorption sites.

Table 2. Isotherms parameters of CFN adsorption

Sample	Isotherms parameters				
	Langmuir				
(I)	q_{max}=464.50	k_L=0.16	Δq_e =3.77	R^2=0.9907	
(II)	q_{max}=356.98	k_L=0.11	Δq_e =5.92	R^2=0.9907	
(III)	q_{max}=300.13	k_L=0.162	Δq_e =4.63	R^2=0.9849	
	Freundlich				
(I)	k_F=165.00	n= 5.99	Δq_e =10.84	R^2=0.9627	
(II)	k_F=173.35	n= 7.88	Δq_e =12.74	R^2=0.8845	
(III)	k_F=134.74	n= 6.86	Δq_e =4.39	R^2=0.9905	
	Dubinin-Raduchkevich				
(I)	q_m=382.24	k_{DR}= $3.58E^{-06}$	E=373.71	Δq_e= 10.34	R^2= 0.6541
(II)	q_m=328.08	k_{DR}= $5.98E^{-06}$	E=298.15	Δq_e= 12.73	R^2= 0.9541
(III)	q_m=284.53	k_{DR}= $5.98E^{-06}$	E=320.42	Δq_e= 8.15	R^2= 0.9534
	Redlich-Peterson				
(I)	a_{RP}=77.97	b_{RP}= 0.224	g=0.9701	Δq_e= 24.94	R^2= 0.9902
(II)	a_{RP}=587.81	b_{RP}= 0.235	g=0.931	Δq_e= 23.61	R^2= 0.9918
(III)	a_{RP}=105.41	b_{RP}= 0.572	g=0.910	Δq_e= 16.05	R^2= 0.9945

q_{max} = (mg g^{-1}); k_L = (L mg^{-1}); k_F = [mg g^{-1} (mg $L^{-1})^{-1/n}$], qm = (mg g^{-1}); k_{DR} = (mol^2 kJ^{-2}); E (KJ mol^{-1}); a_{RP} = (L $mg^{-1})^{g}$; b_{RP} = L g^{-1}; **(I) HDML-ATV; (II) HME4h-ATV; (III) HME48h-ATV**

The Redlich-Peterson model, a three-parameter empirical model combining Langmuir and Freundlich isotherms, shows parameter g close to 1, indicating behavior similar to the Langmuir model for CFN adsorption (Khasri et al., 2018; Wan et al., 2018). The Dubinin-Radushkevich model exhibits high R^2 values (>0.92), suitable for understanding adsorption free energies (E). All three activated hydrochars show E values >8.00 kJ mol^{-1}, suggesting predominant chemisorption.

4 Conclusion

In conclusion, HMDL-ATV, HME4h-ATV, and HME48h-ATV demonstrated varying caffeine adsorption capacities, reflecting their distinct surface properties and suitability for environmental remediation applications.

Acknowledgements

The authors gratefully acknowledge CONCAP and the Universidade Estadual de Maringá (UEM) for their support in providing analytical facilities for this study.

References

[1]Vianna SA, Domenech HLM, Silva RH da, Colombo CA, Pott A. Morphological characterization and productivity estimates of Acrocomia totai Mart. (Arecaceae) – a sustainable alternative of extractivism and cultivation. Rev Bras Frutic . 2021;43(1):e–730.

[2] García Cabrera, Odalys, et al. 'Macauba (Acrocomia Aculeata): Biology, Oil Processing, and Technological Potential'. Oilseed Crops - Uses, Biology and Production, IntechOpen, 8 Mar. 2023. Crossref, doi:10.5772/intechopen.105540..

[3]Souza, Gredson Keiff; Diório, Alexandre; de Lima, Hugo Henrique Carline; dos Santos Maniezzo, Rogerio ; Rinaldi, Andrelson Wellington; Pereira, Nehemias Curvelo; Pomini, Armando Mateus. Assessment of Natural and Post-Extraction Biomass from Acrocomia totai leaves: a Renewable Source of Energy. BioEnergy Research..v.14, p.1025 - 1037, 2020

[4]Y. Wang, M. Jiang, Y. Yang, F. Ran, Hybrid Electrode Material of Vanadium Nitride and Carbon Fiber with Cigarette Butt/Metal Ions Wastes as the precursor for Supercapacitors, Electrochim. Acta. 222 (2016) 1914–1921.

[5]Y. Gao, S. Xu, Q. Yue, Y. Wu, B. Gao, Chemical preparation of crab shell-based activated carbon with superior adsorption performance for dye removal from wastewater, J. Taiwan Inst. Chem. Eng. 61 (2016) 327–335.

[6]Lima, Hugo H.C.; Maniezzo, Rogério S.; Kupfer, Vicente L.; Guilherme, Marcos R.; Moises, Murilo P.; Arroyo, Pedro A.; Rinaldi, Andrelson W.. Hydrochars based on cigarette butts as a recycled material for the adsorption of pollutants. Journal of Environmental Chemical Engineering. v.6, p.7054 - 7061, 2018.